

Intermolecular Forces for the Interaction of H_2O–Graphtriyne Membrane: Contribution of Induction Effects

Noelia Faginas-Lago[1,3(✉)], Yusuf Bramastya Apriliyanto[2], and Andrea Lombardi[1,3]

[1] Dipartimento di Chimica, Biologia e Biotecnologie, Università degli Studi di Perugia, 06123 Perugia, Italy
{noelia.faginaslago,andrea.lombardi}@unipg.it
[2] Department of Chemistry, Indonesia Defense University, Kampus Unhan Komplek IPSC Sentul, 16810 Bogor, Indonesia
[3] Master-tec srl, Via Sicilia 41, 06128 Perugia, Italy

Abstract. Among various carbon allotropes, graphynes are a class of two-dimensional nanosheets, analogous to graphene, that recently have been considered as ideal nanofilters for small gas molecules. In this work, the authors report molecular dynamics (MD) simulations of graphtriyne-H_2O system performed using refined potentials. Intermolecular forces are the key points that govern the adsorption dynamics of gaseous molecules on graphynes surfaces. In order to define the full intermolecular potentials, the Improved Lennard-Jones (ILJ) semi-empirical potential have been subsequently modified by adding an induction term (ind) to take into account the polarizability of H_2O molecules. Evaluation of the computational cost and the distribution of H_2O molecules over graphtriyne membrane have been assessed by comparing the intermolecular forces with and without inclusion of induction potential.

Keywords: Molecular dynamics · Semi-empirical potential energy surface · Gaseous adsorption · Graphynes · DL_POLY software

1 Introduction

Water is one of the most important natural solvent and a by-product of chemical reactions involving energy production either through combustion or respiratory processes. A proper description of H_2O–H_2O intermolecular interactions is essential to study the behaviour of several chemical and biochemical systems towards a better atomistic understanding of a certain system [1,2]. From a chemical point of view, a water molecule can be modeled by a simple point of charge, a tri-atomic system formed by two different atomic constituents, or even higher order site models. These varieties of water models are commonly implemented in the widely used force fields such as UFF and AMBER [3,4]. Despite of this simplicity, H_2O has unusual properties when compared with other similar species.

© Springer Nature Switzerland AG 2021
O. Gervasi et al. (Eds.): ICCSA 2021, LNCS 12958, pp. 426–438, 2021.
https://doi.org/10.1007/978-3-030-87016-4_32

As an example, HF, H_2S and NH_3 molecules are gaseous at atmospheric pressure and room temperature, whereas water is at liquid phase under the same conditions. Moreover, as a liquid, H_2O is rather peculiar because it has a maximum density at about 4 °C and a heat capacity anomalously large. This explains why a considerable research effort is spent to understand water properties (in particular, its ability to form hydrogen bonds, a variety of $(H_2O)_n$ type clusters and to rationalize H_2O–H_2O pairs in terms of intermolecular interactions) [5,6]. Several effective potentials have been developed and implemented in molecular dynamics (MD) calculations with a specific purpose of describing the behaviour of water [7–10].

MD simulations is a theoretical chemistry method for analyzing the movement of atoms and molecules using pre-described potential functions called as force fields. This method can be employed to investigate the structural rearrangement of chemical and biochemical systems such as pure solvents, mixed solutions, gaseous separation and combustion processes [11–14]. However, a generic type of force fields is often limited in its use when studying a particular system, for instance simulation of systems involving water. Aqueous liquid and gaseous phase of H_2O are principally not the same in the description of their total potential energy function. Therefore, researchers interested in a particular system frequently have to partly develop or modify the generic force fields [15–17]. The choice of the modifications must be on the basis of available experimental and/or theoretical data from the literature or prior high level quantum chemical calculations. While the parameterization of force fields is not a simple task, it is crucial for defining a system correctly. One particular system that needed force fields refinement is post-combustion flue gas where H_2O vapour has a significant role on the dynamics of the system [18]. Besides H_2O, post-combustion flue gas contains carbon dioxide which is generally considered as a greenhouse gas. As the emission of carbon dioxide shows an increasing trend during last decades, carbon capture and storage (CCS) attracted global attention in order to mitigate catastrophic effects of global warming [19,20].

In the last few years, various porous materials have been evaluated in their ability to selectively capture gas, especially CO_2 [21–28]. In particular, carbon-based membranes have desirable physicochemical properties (e.g. hydrophobic, chemically inert and thermally stable) and are economically suitable and viable for CCS application [29,30]. The authors of this paper have been recently involved in the study of γ-graphynes using MD tools, specifically the development of force fields related to gas adsorption in that class of carbon allotropes and their analogs [31–34]. γ-graphynes are two-dimensional atomic monolayers where the carbon atoms are arranged in a way that two adjacent hexagons are connected through C-C triple bonds forming uniformly distributed and adjustable nanopores [35]. As nanoporous materials, γ-graphynes are interesting candidates for CCS, particularly in a form of graphtriyne. Graphtriyne is a form of graphynes where each of its benzene ring is connected to each of six others through a chain composed by three acetylenic bonds. Recent reports shows that graphtriyne exhibits high carbon uptake with a relatively good selectivity [36].

A number of force fields have been developed for evaluating the adsorption of gas molecules on different porous materials [37–40]. However, a challenge that have been facing is when dealing with gaseous mixture where H_2O molecules are present [41,42]. A H_2O molecule can induct and alter polarizability of other molecules in its vicinity. This phenomenon indeed changes the intermolecular forces description between the molecules. Therefore, an additional term is needed to be included to the total potentials to solve this issue. However, as a consequence, this additional term will increase the computational cost. The incomplete description of the full intermolecular potentials can partially be fixed by the inclusion of an induction term [9,10]. In this work, MD simulations were performed involving a graphtriyne membrane and an amount of H_2O molecules in gas phase in an attempt to evaluate the distribution of H_2O molecules over graphtriyne membrane and the computational cost for system with and without inclusion of induction potential.

In the following section, theoretical methods and construction of the present potential energy functions are outlined. The discussions regarding the results and improvements of the molecular simulations code are presented in the Sect. 3, while in the Sect. 4 the paper brings up concluding remarks.

2 Methods

The intermolecular forces of interest in this work are those occured between H_2O molecules pair and between the H_2O and the graphtriyne membrane. The intermolecular interaction energy is further decomposed in terms of molecule-molecule pair contribution, which are non-electrostatic and electrostatic contributions.

$$V_{tot}(r) = V_{nonelec} + V_{elec} \tag{1}$$

The non-electrostatic contribution ($V_{nonelec}$) is measured by taking into consideration the strength of induced dipoles and the average molecular sizes. This can be done by assigning a value of polarizability to the both interacting centers. On the other hand, the electrostatic contribution (V_{elec}) is evaluated by employing the Coulomb's law. $V_{nonelec}$ is given by the following equation

$$V_{nonelec}(r) = V_{ILJ} + V_{ind} \tag{2}$$

where the non-inductive part of the non-electrostatic contribution is expressed by adopting the Improved Lennard-Jones (ILJ) potential [43–47].

$$V_{ILJ}(r) = \varepsilon \left[\frac{m}{n(r) - m} \left(\frac{r_0}{r} \right)^{n(r)} - \frac{n(r)}{n(r) - m} \left(\frac{r_0}{r} \right)^{m} \right] \tag{3}$$

In Eq. 3, ε, r_0 and m are parameters specific to the involved molecular pair, and r is the distance between the two interacting centers of the same molecular pair. m indicates the type of interaction where its value is 6 for neutral-neutral pairs, 4 for ion-neutral pair and 1 for ion-ion pairs. In order to control the

decline of the repulsion and the strength of the attraction in Eq. 3, the $n(r)$ term is employed (Eq. 4).

$$n(r) = \beta + 4.0 \left(\frac{r}{r_0} \right)^2 \tag{4}$$

In Eq. 4, β is a factor that modulates the hardness of the interacting pair [48,49]. This newly introduced parameter is what makes ILJ potential (Eq. 3) able to indirectly take into account some effects of atom clustering, induction and charge transfer and to improve the Lennard-Jones function at asymptotic regions. Nevertheless, while ILJ improves the description of the present system, other effects should be included in the intermolecular potential for enhancing the model of the system.

It should be considered that charge transfer and induction effects may be important in the interaction between H_2O–H_2O molecules. The H_2O–H_2O interaction can be well defined by using a single effective dispersion + induction center ($V_{ILJ} + V_{ind}$) as already mentioned in (Eq. 2). A careful separate characterization of each of these contributions was performed. Charge transfer effects in the perturbative limit were taken into account indirectly inside the ILJ part by lowering the value of β as discussed, for instance, in Ref. [31]. As for the induction term (V_{ind}), commonly, its contribution to the total interaction is quite small. However, we decided to include it (Eq. 2) in order to quantify its average contribution to the total intermolecular interaction in the water pair interaction and water-graphtriyne interaction, using the single term (in meV) as follows [50].

$$V_{ind}(r) = -4.0\, C \mu^2 \alpha / R^6 \tag{5}$$

In Eq. 5 μ and α are the dipole moment and the polarizability of H_2O expressed in debye (D) and $Å^3$, respectively. R is the distance between the center of mass of each H_2O pair given in Å. This distance is assumed to be coincident with the Ow–Ow separation (Fig. 1), while C is a constant equal to 316.14 to convert the potential in meV unit.

Figure 1 shows the geometrical details of the molecular models employed in this work. A model taken from Ref. [10] was used to represent the water molecule. In this model, the charge is distributed in a way that corresponds to the dipole moment of water in the gas phase (2.1 D) [9]. Each of these point charges is centered in the atoms composing water molecule. The membrane structure was taken from Ref. [36], and had been previously optimized through periodic DFT calculations. For the MD simulations, the membranes were set as a frozen framework while H_2O molecules were set as rigid structures. The MD simulations were performed in simulation boxes with dimensions 72.210 Å× 62.523 Å× 280.0 Å. Inside each box, a graphtriyne membrane with dimensions 72.210 Å× 62.523 Å was placed. Simulations were performed uniquely at the temperature of 333 K. The gas molecules were randomly distributed with equal amount into each region of the box yielding a bulk density of H_2O about 3.1526×10^{-2} mol L^{-1}. Figure 2 shows the relative sizes of H_2O molecules, the graphtryine membrane and the simulation box in a qualitative view.

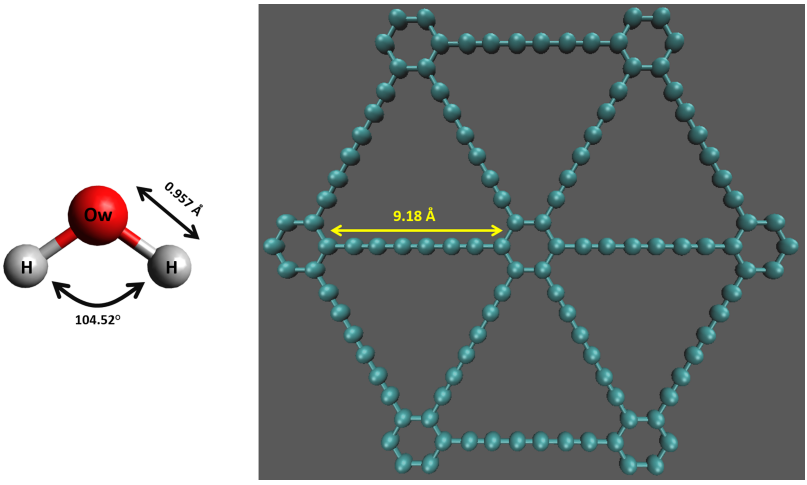

Fig. 1. Structural details of the molecular models of water and graphtryine membrane.

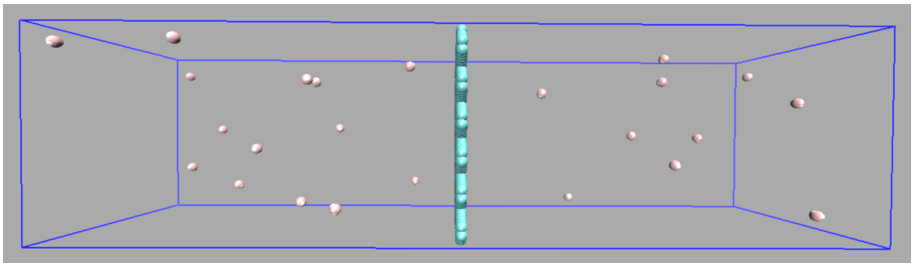

Fig. 2. A screenshot of the simulation box filled with H_2O molecules where the graphtriyne layer is located in the middle of the box.

All MD simulations were performed using the DL_POLY 2 package [51] at canonical NVT ensemble using the Nose-Hoover thermostat and periodic boundary conditions applied in all directions. The ILJ potential and the electrostatic interactions cutoff distances were set to 15 Å, where the electrostatic part was calculated by using the Ewald method. At first, two short simulations were performed by using ILJ and ILJ coupled with induction. Both lasted 2.2 ps after 0.2 ps of equilibration period with a time step of 1 fs. Thereafter, other two longer calculations (2 ns after 0.2 ns equilibration) were run in order to analyze the distribution of H_2O molecules and the corresponding energy contributions. The simulations were performed before and after a modification in some particular routines. Values of relevant parameters are given in Table 1.

Table 1. Parameters for the non-electrostatic interactions (ILJ) of water–water and water–graphtriyne membrane.

Interacting pair	ϵ $(kcal\ mol^{-1})$	r_0 $(\mathring{A})$	β	m
Ow–Ow	0.2089	3.730	6.6	6.0
Ow–C	0.1845	3.712	6.5	6.0

3 Computational Results

We have incorporated some modified routines to include the induction (ind) contribution into the full intermolecular interaction. The modification was done mainly in a routine of the DL_POLY2 package called *forces_modules.f* that handles all interatomic forces using the verlet neighbour list. The *forces_modules.f* is a piece of code that calls other subroutines to calculate the intermolecular forces for each interacting pair of the system. The subsequent subroutines brought by *forces_modules.f* depend on the choice of the predefined potential. *Ewald1* subroutine will be called for ILJ potential, while *ewaldm1* and *induct* subroutines will be called for ILJ+ind potential. The *ewaldm1* and *induct* subroutines were written in order to take into account the electrostatic forces and the induction forces itself, respectively. These subroutines are located in *ewald_module.f* and *coulomb_module.f*. The difference between *ewaldm1* and the original *ewald1* is that the *ewaldm1* subroutine takes into account the point charges distribution which often altered by the induction processes.

A small modification to the above mentioned subroutines had also been done in the previous report [42]. It was reported that the modification had a considerable impact on the total simulation time. As already reported there that, initially, the total CPU time for the ILJ+ind potential took about five times longer than simulation with only the ILJ potential. After a small modification, the difference in total CPU time decreases to about four times between the two potentials. The reported simulations were conducted for 600 fs, accordingly, longer simulation time would has considerable impact on the total CPU time. It was then concluded that something inside the *ewaldm1* and *induct* subroutines that made the simulations took more time than the *ewald1* subroutine applied for ILJ only.

The aim of this work is to evaluate MD simulations codes and results reported in the previous publication [42], thus further improvement of the code can bring us more efficient computational time with reasonable statistical results. At this point, the authors have performed further analysis to the subroutines and simulations results reported in the ICCSA 2019 and 2020 papers [18,42] where a system of $CO_2/N_2/H_2O$ gaseous mixture was simulated without and with induction potential, respectively. The authors find that the most time consuming of the ILJ+ind potential code is the calculation of electrostatic contributions after

induction occurs (particularly, inside the *ewaldm1* subroutine), not in the van der Waals (non-electrostatic) part. It should be noted that Refs. [9,10] indicate that the total dipole moment of H_2O is varying from 2.1 D (H_2O–H_2O pair) to 1.85 D (H_2O–CO_2/N_2 pair). Therefore, the dipole moment of H_2O is not a single value (hence the atomic charges of H_2O are also varying). It's values depend on which molecules interact with H_2O. In order to account for the flexibility of H_2O atomic charges, the authors wrote 3 Fourier cycles inside the *ewaldm1* subroutine.

These 3 Fourier cycles were inspired by the counterpoise method. The authors handled the interchange of H_2O atomic charges (total dipole moment from 1.85 D to 2.1 D) by calculating the electrostatic contribution in *ewaldm1* subroutine as follows:

Fourier 1: total electrostatic term for all interacting pairs, where the atomic charges of H_2O correspond to 1.85 D (as provided in the FIELD input file).

Fourier 2: electrostatic term for interaction involving only H_2O–H_2O pairs, where the atomic charges of H_2O correspond to 1.85 D.

Fourier 3: electrostatic term for interaction involving only H_2O–H_2O pairs, where the atomic charges of H_2O correspond to 2.10 D.

Consequently, the total electrostatic contribution from the *ewaldm1* is Fourier 1 - Fourier 2 + Fourier 3. These Fourier terms are needed only if periodic boundary conditions (PBC) are applied. This approach has proven energetically can recover the interchange of atomic charge as the effect of induction. Unfortunately, this separation of Fourier cycles is the reason why the computational time is quite high for ILJ+ind potential.

Up to this paper is being written, the authors are still searching an alternative way to solve the electrostatic contribution of ILC+ind potential (*ewaldm1*) in a single Fourier cycle without altering too much the original code, while adapting the establihed architecture and workflow of DL_POLY2 package. However, we have made an improvement to *forces_modules.f* in a way that this code can evaluate the simulations systems whether in a form of pure or mixture systems. Furthermore, we present a code modification by introducing conditional statement to only perform a single Fourier transform (*ewald1*) for pure system in order to make the program run more efficient. It is worth to note here that, before modification, the total CPU time is quite high for the case of pure CO_2 system (ILJ+induction) [42]. It is four times longer than the same system with ILJ potential for only 600 steps. For pure CO_2 with ILJ+induction, the CPU time is almost even close to the CPU time for mixture system. We know that since pure systems are not as complex as mixtures, the computational time for pure system should not approach the mixture systems if their total steps are the same. After modification, we report that the total CPU time for simulation of pure H_2O system with and without induction are quite fast and do not

significantly different for 2.2 ps (2200 steps) simulations (Table 2). This trend in CPU time will hold for all pure gaseous systems. Moreover, the energy contributions for 2.2 ps simulations are similar and the inclusion of induction potential does not much altering the average of configuration energy (PES). Table 2 shows the comparison of CPU time and statistical analysis of MD simulations results for pure H_2O systems with and without induction.

Table 2. Total CPU time and statistical energy contribution of MD simulations. The energy for the simulations with shorter MD time is reported in unit of 10^{-2} kcal mol^{-1}.

Potential	Time		Energy ($kcal\ mol^{-1}$)		
	MD (ps)	CPU (s)	Configuration	vdW	Coulombic
ILJ	2.2	148.768	-2.637 ± 7.990	-1.234 ± 0.112	-1.403 ± 7.994
	2000	32786.587	-5.266 ± 2.604	-3.865 ± 2.402	-1.402 ± 1.965
ILJ+ind	2.2	151.778	-2.683 ± 7.990	-1.279 ± 0.142	-1.404 ± 7.995
	2000	62725.082	-3.773 ± 7.146	-0.631 ± 2.446	-3.142 ± 6.999

In our case, we are interested in introducing the induction term for the contributions related with the water interaction pairs and water-membrane interactions. Indeed, 2.2 ps simulations are not sufficient in order to describe quantitatively the dynamics of the systems. Therefore, we perform further MD simulations with total simulation time of 2000 ps. From the Table 2 we can see that the CPU time for ILJ+ind is about two times from the ILJ only. Judging from the CPU time, this result is better than the previous reported result [42]. This is a good indication that an improvement of the code's efficiency has been achieved. Although the inclusion of induction potential has fairly small contribution to the total potential (configuration) energy for short time MD simulations (2.2 ps), this small energy contribution is accumulated at much longer simulation (2000 ps), producing quite different statistical energy contributions (see Table 2). As the result, the dynamical process of the system can be considerably affected and induction potential starts to get much more important role to the systems. Furthermore, to assess the impact of induction term to the dynamical process of the system, we also evaluated the distribution of H_2O molecules on graphtriyne as well as the distribution between H_2O molecules. The distribution of H_2O molecules from the surface of graphtriyne is represented by the z-density, in which the density of H_2O as a function of z axis relative to the graphtriyne position is reported. Meanwhile, intermolecular distribution between H_2O molecules is represented by the radial distribution function, which is the probability of a water molecule to have other water molecules as neighbors at a certain distance. The radial distribution functions (RDFs) and z-density profiles for 2000 ps simulation time are presented in Fig. 3.

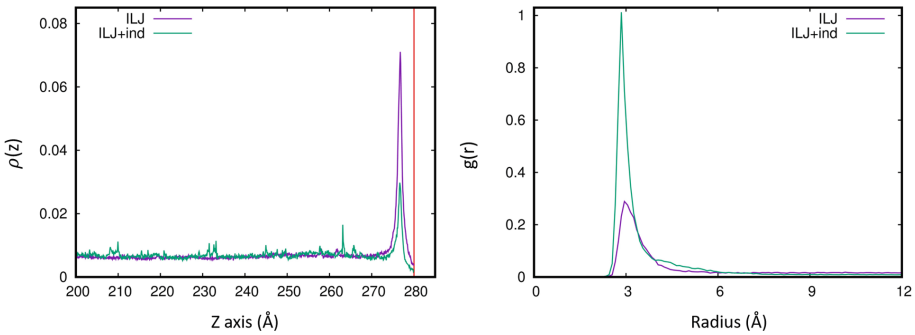

Fig. 3. z-density profiles (left panel) and radial distribution functions of H_2O–H_2O (right panel) for the simulations using ILJ and ILJ+ind potentials. The red vertical line represent the position of graphtriyne layer. The reported values have been normalized. (Color figure online)

Figure 3 shows that the inclusion of induction term has considerably significant impact to the system. The H_2O molecules tend to prefer interacting with each other after the introduction of induction potential. This phenomenon can be seen in the RDFs. The ILJ+ind has higher peak meaning that more H_2O molecules are located near a certain H_2O molecule. As a consequence, the interaction between H_2O–graphtriyne tend to decrease for the case of the ILJ+ind potential, yielding a lower peak in the z-density profile. It should be noted that these results are obtained at 2 ns simulation time. However, running MD simulations for 2 ns is not long enough for estimating quantitative results. In order to yield much more representative data, a simulation higher than five nanoseconds is more adequate. Nevertheless, by introducing some modifications to the code, we improved the performance of ILJ+ind code so that CPU time could be reduced significantly. We also proofed that the induction potential played an important role and contributed to the dynamics of the system. In future works, further improvements are needed to be made to the code to have a faster running simulation using ILJ+ind potential, especially for mixture systems.

4 Conclusions

The induction term has been introduced into the internal DL_POLY2 code in order to improve the description of intermolecular forces and to evaluate H_2O distribution on graphtriyne surface as well as the corresponding computational cost. A considerable impact on the total CPU time has been observed for pure gaseous systems both for ILJ and ILJ+ind potentials after modifications to the existing code. The inclusion of induction potential has fairly small contribution to the total potential energy for short time MD simulations. However, this small energy contribution can be accumulated for much longer simulation time, thus the dynamical process of the system can be considerably affected. Future modifications in the *ewaldm1* subroutine are expected to diminish CPU time even

further for calculations with ILJ+ind potential for pure and mixture systems. That way, future MD simulations with larger quantities of molecules and even longer simulation time will be accessible thus the system will be described better than with only ILJ potential.

Acknowledgements. N. F.-L and A. L. thank the MIUR and the University of Perugia for the financial support of the AMIS project through the "Dipartimenti di Eccellenza" program. N. F.-L also acknowledges the Fondo Ricerca di Base 2020 (RICBASE2020FAGINAS) del Dipartimento di Chimica, Biologia e Biotecnologie della Università di Perugia for financial support and the Herla Project for allocated computing time. A. L. acknowledges financial support from MIUR PRIN 2015 (contract 2015F59J3R 002).

References

1. Faginas-Lago, N., Lombardi, A., Albertí, M., Grossi, G.: Accurate analytic intermolecular potential for the simulation of Na^+ and K^+ ion hydration in liquid water. J. Mol. Liq. **204**, 192–197 (2015). https://doi.org/10.1016/j.molliq.2015.01.029
2. Faginas-Lago, N., Albertí, M., Laganà, A., Lombardi, A.: Ion-water cluster molecular dynamics using a semiempirical intermolecular potential. In: Gervasi, O., et al. (eds.) ICCSA 2015. LNCS, vol. 9156, pp. 355–370. Springer, Cham (2015). https://doi.org/10.1007/978-3-319-21407-8_26
3. Rappe, A.K., Casewit, C.J., Colwell, K.S., Goddard, W.A., Skiff, W.M.: UFF, a full periodic table force field for molecular mechanics and molecular dynamics simulations. J. Am. Chem. Soc. **114**(25), 10024–10035 (1992). https://doi.org/10.1021/ja00051a040
4. Pearlman, D., et al.: AMBER, a package of computer-programs for applying molecular mechanics, normal-mode analysis, molecular-dynamics and free-energy calculations to simulate the structural and energetic properties of molecules. Comput. Phys. Commun. **91**, 1–41 (1995). https://doi.org/10.1016/0010-4655(95)00041-D
5. Faginas-Lago, N., Albertí, M., Laganà, A., Lombardi, A.: Water $(H_2O)_m$ or benzene $(C_6H_6))_n$ aggregates to solvate the K^+? In: Murgante, B., Misra, S., Carlini, M., Torre, C.M., Nguyen, H.Q., Taniar, D., Apduhan, B.O., Gervasi, O. (eds.) Computational Science and Its Applications -ICCSA 2013, pp. 1–15. Springer, Berlin Heidelberg (2013). https://doi.org/10.1007/978-3-642-39637-3_1
6. Lago, N.F., Albertí, M., Laganà, A., Lombardi, A., Pacifici, L., Costantini, A.: The molecular stirrer catalytic effect in methane ice formation. In: Murgante, B., et al. (eds.) ICCSA 2014. LNCS, vol. 8579, pp. 585–600. Springer, Cham (2014). https://doi.org/10.1007/978-3-319-09144-0_40
7. Das, A.K., et al.: Development of an advanced force field for water using variational energy decomposition analysis. J. Chem. Theory Comput. **15**(9), 5001–5013 (2019). https://doi.org/10.1021/acs.jctc.9b00478
8. Wang, H., Yang, W.: Force field for water based on neural network. J. Phys. Chem. Lett. **9**(12), 3232–3240 (2018). https://doi.org/10.1021/acs.jpclett.8b01131
9. Albertí, M., Pirani, F., Laganà, A.: Carbon dioxide clathrate hydrates: selective role of intermolecular interactions and action of the SDS catalyst. J. Phys. Chem. A **117**(32), 6991–7000 (2013). https://doi.org/10.1021/jp3126158

10. Albertí, M., Aguilar, A., Cappelletti, D., Laganà, A., Pirani, F.: On the development of an effective model potential to describe water interaction in neutral and ionic clusters. Int. J. Mass Spectrom. **280**, 50–56 (2009). https://doi.org/10.1016/j.ijms.2008.07.018
11. Liu, B., Smit, B.: Molecular simulation studies of separation of CO_2/N_2, CO_2/CH_4, and CH_4/N_2 by ZIFs. J. Phys. Chem. C **114**(18), 8515–8522 (2010). https://doi.org/10.1021/jp101531m
12. Faginas-Lago, N., Albertí, M., Costantini, A., Laganà, A., Lombardi, A., Pacifici, L.: An innovative synergistic grid approach to the computational study of protein aggregation mechanisms. J. Mol. Model. **20**(7), 2226 (2014). https://doi.org/10.1007/s00894-014-2226-4
13. Rampino, S., Faginas-Lago, N., Laganà, A., Huarte-Larrañaga, F.: An extension of the grid empowered molecular simulator to quantum reactive scattering. J. Comput. Chem. **33**(6), 708–714 (2012). https://doi.org/10.1002/jcc.22878
14. Lombardi, A., Faginas-Lago, N., Laganà, A.: Grid calculation tools for massive applications of collision dynamics simulations: carbon dioxide energy transfer. In: Murgante, B., et al. (eds.) ICCSA 2014. LNCS, vol. 8579, pp. 627–639. Springer, Cham (2014). https://doi.org/10.1007/978-3-319-09144-0_43
15. Lombardi, A., Faginas-Lago, N., Pacifici, L., Grossi, G.: Energy transfer upon collision of selectively excited CO_2 molecules: State-to-state cross sections and probabilities for modeling of atmospheres and gaseous flows. J. Chem. Phys. **143**(3), 034307 (2015). https://doi.org/10.1063/1.4926880
16. Faginas-Lago, N., Lombardi, A., Pacifici, L., Costantini, A.: Design and implementation of a grid application for direct calculations of reactive rates. Comput. Theor. Chem. **1022**, 103–107 (2013). https://doi.org/10.1016/j.comptc.2013.08.014
17. DuBay, K.H., Hall, M.L., Hughes, T.F., Wu, C., Reichman, D.R., Friesner, R.A.: Accurate force field development for modeling conjugated polymers. J. Chem. Theory Comput. **8**(11), 4556–4569 (2012). https://doi.org/10.1021/ct300175w
18. Faginas-Lago, N., Apriliyanto, Y.B., Lombardi, A.: Molecular simulations of $CO_2/N_2/H_2O$ gaseous mixture separation in graphtriyne membrane. In: Misra, S., et al. (eds.) ICCSA 2019. LNCS, vol. 11624, pp. 374–387. Springer, Cham (2019). https://doi.org/10.1007/978-3-030-24311-1_27
19. Smit, B.: Carbon capture and storage: introductory lecture. Faraday Discuss. **192**, 9–25 (2016). https://doi.org/10.1039/C6FD00148C
20. Bui, M., et al.: Carbon capture and storage (CCS): the way forward. Energy Environ. Sci. **11**, 1062–1176 (2018). https://doi.org/10.1039/C7EE02342A
21. Srinivas, G., Krungleviciute, V., Guo, Z.X., Yildirim, T.: Exceptional CO_2 capture in a hierarchically porous carbon with simultaneous high surface area and pore volume. Energy Environ. Sci. **7**, 335–342 (2014). https://doi.org/10.1039/C3EE42918K
22. Ghosh, S., Sevilla, M., Fuertes, A.B., Andreoli, E., Ho, J., Barron, A.R.: Defining a performance map of porous carbon sorbents for high-pressure carbon dioxide uptake and carbon dioxide-methane selectivity. J. Mater. Chem. A **4**, 14739–14751 (2016). https://doi.org/10.1039/C6TA04936B
23. Kim, J., Lin, L.C., Swisher, J.A., Haranczyk, M., Smit, B.: Predicting large CO_2 adsorption in aluminosilicate zeolites for postcombustion carbon dioxide capture. J. Am. Chem. Soc. **134**(46), 18940–18943 (2012). https://doi.org/10.1021/ja309818u
24. Lin, L.C., et al.: Understanding CO_2 dynamics in metal-organic frameworks with open metal sites. Angew. Chem. Int. Ed. **52**(16), 4410–4413 (2013). https://doi.org/10.1002/anie.201300446

25. Schrier, J.: Carbon dioxide separation with a two-dimensional polymer membrane. ACS Appl. Mater. Interfaces. **4**(7), 3745–3752 (2012). https://doi.org/10.1021/am300867d
26. Xiang, Z., et al.: Systematic tuning and multifunctionalization of covalent organic polymers for enhanced carbon capture. J. Am. Chem. Soc. **137**(41), 13301–13307 (2015). https://doi.org/10.1021/jacs.5b06266
27. Liu, H., et al.: A hybrid absorption-adsorption method to efficiently capture carbon. Nat. Commun. **5**, 5147 (2014). https://doi.org/10.1038/ncomms6147
28. Apriliyanto, Y.B., Darmawan, N., Faginas-Lago, N., Lombardi, A.: Two-dimensional diamine-linked covalent organic frameworks for co 2/n 2 capture and separation: theoretical modeling and simulations. Phys. Chem. Chem. Phys. **22**(44), 25918–25929 (2020). https://doi.org/10.1039/D0CP04258G
29. Bartolomei, M., Carmona-Novillo, E., Giorgi, G.: First principles investigation of hydrogen physical adsorption on graphynes' layers. Carbon **95**, 1076–1081 (2015). https://doi.org/10.1016/j.carbon.2015.08.118
30. Ganesan, A., Shaijumon, M.: Activated graphene-derived porous carbon with exceptional gas adsorption properties. Microporous Mesoporous Mater. **220**, 21–27 (2015). https://doi.org/10.1016/j.micromeso.2015.08.021
31. Apriliyanto, Y.B., et al.: Nanostructure selectivity for molecular adsorption and separation: the case of graphyne layers. J. Phys. Chem. C **122**(28), 16195–16208 (2018). https://doi.org/10.1021/acs.jpcc.8b04960
32. Faginas-Lago, N., Yeni, D., Huarte, F., Wang, Y., Alcamí, M., Martin, F.: Adsorption of hydrogen molecules on carbon nanotubes using quantum chemistry and molecular dynamics. J. Phys. Chem. A **120**(32), 6451–6458 (2016). https://doi.org/10.1021/acs.jpca.5b12574
33. Yeamin, M.B., Faginas-Lago, N., Albertí, M., García Cuesta, I., Sánchez-Marín, J., Sánchez de Merás, A.: Multi-scale theoretical investigation of molecular hydrogen adsorption over graphene: coronene as a case study. RSC Adv. **4**, 54447–54453 (2014). https://doi.org/10.1039/C4RA08487J
34. Faginas-Lago, N., Apriliyanto, Y.B., Lombardi, A.: Confinement of co_2 inside carbon nanotubes. Eur. Phys. J. D **75**(161), 1–10 (2021). https://doi.org/10.1140/epjd/s10053-021-00176-7
35. James, A., et al.: Graphynes: indispensable nanoporous architectures in carbon flatland. RSC Adv. **8**, 22998–23018 (2018). https://doi.org/10.1039/C8RA03715A
36. Bartolomei, M., Giorgi, G.: A novel nanoporous graphite based on graphynes: First-principles structure and carbon dioxide preferential physisorption. ACS Appl. Mater. Interfaces. **8**(41), 27996–28003 (2016). https://doi.org/10.1021/acsami.6b08743
37. Lim, J.R., Yang, C.T., Kim, J., Lin, L.C.: Transferability of CO_2 force fields for prediction of adsorption properties in all-silica zeolites. J. Phys. Chem. C **122**(20), 10892–10903 (2018). https://doi.org/10.1021/acs.jpcc.8b02208
38. Boyd, P.G., Moosavi, S.M., Witman, M., Smit, B.: Force-field prediction of materials properties in metal-organic frameworks. J. Phys. Chem. Lett. **8**(2), 357–363 (2017). https://doi.org/10.1021/acs.jpclett.6b02532
39. Lin, L.C., Lee, K., Gagliardi, L., Neaton, J.B., Smit, B.: Force-field development from electronic structure calculations with periodic boundary conditions: applications to gaseous adsorption and transport in metal-organic frameworks. J. Chem. Theory Comput. **10**(4), 1477–1488 (2014). https://doi.org/10.1021/ct500094w

40. Vekeman, J., García Cuesta, I., Faginas-Lago, N., Wilson, J., Sánchez-Marín, J., Sánchez de Merás, A.: Potential models for the simulation of methane adsorption on graphene: development and CCSD(T) benchmarks. Phys. Chem. Chem. Phys. **20**(39), 25518–25530 (2018). https://doi.org/10.1039/C8CP03652G
41. Faginas-Lago, N., Apriliyanto, Y.B., Lombardi, A.: Carbon capture and separation from $CO_2/N_2/H_2O$ gaseous mixtures in bilayer graphtriyne: a molecular dynamics study. In: Gervasi, O., et al. (eds.) ICCSA 2020. LNCS, vol. 12255, pp. 489–501. Springer, Cham (2020). https://doi.org/10.1007/978-3-030-58820-5_36
42. de Aragão, E.V.F., Faginas-Lago, N., Apriliyanto, Y.B., Lombardi, A.: Gas adsorption on graphtriyne membrane: impact of the induction interaction term on the computational cost. In: Gervasi, O., et al. (eds.) ICCSA 2020. LNCS, vol. 12255, pp. 513–525. Springer, Cham (2020). https://doi.org/10.1007/978-3-030-58820-5_38
43. Pirani, P., Brizi, S., Roncaratti, L., Casavecchia, P., Cappelletti, D., Vecchiocattivi, F.: Beyond the Lennard-Jones model: a simple and accurate potential function probed by high resolution scattering data useful for molecular dynamics simulations. Phys. Chem. Chem. Phys. **10**, 5489–5503 (2008). https://doi.org/10.1039/B808524B
44. Lombardi, A., Laganà, A., Pirani, F., Palazzetti, F., Lago, N.F.: Carbon oxides in gas flows and earth and planetary atmospheres: state-to-state simulations of energy transfer and dissociation reactions. In: Murgante, B., et al. (eds.) ICCSA 2013. LNCS, vol. 7972, pp. 17–31. Springer, Heidelberg (2013). https://doi.org/10.1007/978-3-642-39643-4_2
45. Faginas-Lago, N., Albertí, M., Lombardi, A., Pirani, F.: A force field for acetone: the transition from small clusters to liquid phase investigated by molecular dynamics simulations. Theor. Chem. Acc. **135**(7), 1–9 (2016). https://doi.org/10.1007/s00214-016-1914-9
46. Lombardi, A., Faginas-Lago, N., Gaia, G., Federico, P., Aquilanti, V.: Collisional energy exchange in CO_2–N_2 gaseous mixtures. In: Gervasi, O., et al. (eds.) ICCSA 2016. LNCS, vol. 9786, pp. 246–257. Springer, Cham (2016). https://doi.org/10.1007/978-3-319-42085-1_19
47. Albertí, M., Faginas-Lago, N.: Ion size influence on the ar solvation shells of $M^+C_6F_6$ clusters (M = Na, K, Rb, Cs). J. Phys. Chem. A **116**(12), 3094–3102 (2012). https://doi.org/10.1021/jp300156k
48. Pirani, F., Albertí, M., Castro, A., Moix Teixidor, M., Cappelletti, D.: Atom-bond pairwise additive representation for intermolecular potential energy surfaces. Chem. Phys. Lett. **394**(1–3), 37–44 (2004). https://doi.org/10.1016/j.cplett.2004.06.100
49. Pacifici, L., Verdicchio, M., Faginas-Lago, N., Lombardi, A., Costantini, A.: A high-level ab initio study of the $N_2 + N_2$ reaction channel. J. Comput. Chem. **34**(31), 2668–2676 (2013). https://doi.org/10.1002/jcc.23415
50. Albertí, M., et al.: Small water clusters: the cases of rare gas-water, alkali ion-water and water dimer. In: Gervasi, O., Murgante, B., Laganà, A., Taniar, D., Mun, Y., Gavrilova, M.L. (eds.) ICCSA 2008. LNCS, vol. 5072, pp. 1026–1035. Springer, Heidelberg (2008). https://doi.org/10.1007/978-3-540-69839-5_78
51. Smith, W., Yong, C., Rodger, P.: `DL_POLY`: application to molecular simulation. Mol. Simul. **28**(5), 385–471 (2002)